JOURNAL OF CATALYSIS 66, 82–92 (1980)

The Role of Nickel in the Activity of Unsupported Ni–Mo Hydrodesulfurization Catalysts

KERRY C. PRATT, JOHN V. SANDERS, AND NICHOLAS TAMP

CSIRO Division of Materials Science, Catalysis and Surface Science Laboratory, University of Melbourne, Parkville, Victoria 3052, Australia

Received December 20, 1979; revised April 14, 1980

A series of unsupported nickel–molybdenum sulfide catalysts covering the range 0–100 atom% nickel has been prepared by continuous coprecipitation. The catalyst containing 55 atom% nickel showed the highest specific activity for thiophene hydrodesulfurization. Chemical and structural analyses of the catalysts appear consistent with the suggestion that the hydrodesulfurization sites are coordinatively unsaturated Mo^{3+} cations at anion vacancies on the edges of the MoS_2 flakes, while edge-intercalated nickel serves as an olefin hydrogenation site, and in reducing Mo^{4+} to Mo^{3+}, in accordance with the structural model of Cossee and Farragher. Highly dispersed Ni_3S_2 is suggested to play a role in hydrogen activation, transferring protons and electrons to the MoS_2, and this may form the origin of the synergistic mechanism. The likely roles of the promoter are summarized.

INTRODUCTION

Catalysts based on molybdenum or tungsten, promoted by nickel or cobalt, have been used extensively for hydrodesulfurization (HDS) in petroleum refining for many years. More recently, sulfide catalysts have been reapplied to the hydrogenation of coal and the hydrotreating of coal tars and shale oils. In spite of the great commercial significance of these catalysts and the many investigations made to date, the exact mechanism of hydrogenolysis of sulfur-containing aromatics and the structure of the operating catalyst are incompletely understood. Of the current structural theories for the operating catalyst, the pseudointercalation model (*1, 2*), the synergistic model (*3, 4*), and the importance of semiconducting properties of the catalyst (*5*) have gained the widest acceptance. These models are not necessarily mutually exclusive, and none is entirely satisfactory. In particular, the pseudointercalation model and the semiconductivity ideas do not explain the large amounts of promoter which must be added to achieve maximum activity. The synergistic model still awaits a proper mechanistic explanation. The support is considered only as a diluent, and only the monolayer model (*6*) now championed by Massoth (*7*) assigns a role to the support.

In this paper we describe the first results in a series of experiments directed toward understanding the role of the promoter and the mechanism of the transition from the oxidic precursor to the sulfided form of the catalyst. We chose to investigate the Ni–Mo system, since this has received less attention than the Co–Mo catalyst, and appears likely to become more important in coal, shale oil, and residua processing, where a full range of hydrorefining reactions is required, rather than just desulfurization. Scientific development of sulfide catalysts especially for oxygen and nitrogen removal, and hydrocracking, will benefit from a proper knowledge of the mode of operation of existing HDS catalysts. In the first instance we have employed unsupported catalysts, in order to avoid ambiguities introduced by the support. The objective of the initial part of the program was to investigate the relationship between the composition of the unsupported catalysts

0021-9517/80/110082-11$02.00/0

and their structure and activity. We are aware of only two other studies covering a range of unsupported Ni–Mo catalysts (*8–10*), which have appeared recently.

EXPERIMENTAL

(*i*) *Catalyst Preparation*

The aim was to produce as a starting material a series of intimately dispersed mixed oxides covering the range 0–100 atom% Ni. A continuous coprecipitation technique similar to that described by Andrushkevich *et al.* (*11*) was employed. This method of preparation differs from those used in the recent studies of the unsupported Ni–Mo system (*8–10*), and thus provides a useful comparison of the influence of catalyst preparation technique. Aqueous solutions of $Ni(NO_3)_2 \cdot 6H_2O$ (Analar) and $(NH_4)_6Mo_7O_{24} \cdot 4H_2O$ (Analar) containing ammonia (to convert the Mo to MoO_4^{2-}) were continuously mixed in a stirred vessel at 80°C. Composition of the precipitate was controlled by choice of concentrations and flow rates of the two solutions. Total flow rate was chosen to give a residence time of about 1 hr in the stirred vessel for precipitate aging. The precipitate was removed continuously, and washed in cold distilled water until no free nickel was detectable. This was followed by drying overnight at 120°C, and finally by calcination in air at 400°C for 4 hr. This technique was chosen as it provides a uniform precipitate as a starting material, and it was felt that the procedure above should duplicate most closely the commercial procedures used in manufacturing supported industrial catalysts. The pure molybdenum sample was prepared by precipitation from a solution of $(NH_4)_6Mo_7O_{24} \cdot 4H_2O$ by nitric acid addition. Metals content of the resulting catalysts was determined by atomic absorption spectroscopy. Details of the catalysts prepared are given in Table 1.

TABLE 1

Details of Catalysts

Catalyst	$\frac{Ni}{Ni + Mo}$ (atomic ratio)	Appearance (oxidic phase)
A	0	Pale green
B	0.30	Olive green
C	0.41	Olive green
D	0.55	Mustard
E	0.73	Black
F	0.79	Black
G	0.92	Black
H	1.0	Black

(*ii*) *Catalyst Testing*

Catalysts were evaluated according to their activity for thiophene hydrogenolysis at near-atmospheric pressure and at four temperatures, nominally 523, 548, 573, and 598 K. The microreactor consisted of a 9-mm-i.d. stainless-steel tube (Type 316) externally heated. For each run about 0.5 g of catalyst (size range 80–100 mesh), diluted with an equal volume of ground Pyrex glass, was used in the reactor. The feedstream to the reactor was hydrogen, saturated with thiophene (Hopkin and Williams) at 0°C, which resulted in a feed composition of about 3 vol% thiophene in hydrogen. Flow rates covered the range 0–50 ml/min, at STP. Prior to reaction, the catalyst was presulfided *in situ* with a 20 vol% mixture of H_2S in hydrogen for 4 hr at 400°C. Reaction products were analyzed by on-line gas chromatography for thiophene and C_4 hydrocarbons. Some care is needed in the chromatographic analysis, and exact details have been published elsewhere (*12*).

Steady-state catalysts for various analyses were prepared by sulfiding, reacting for 6 hr at 595 K, cooling under reaction atmosphere, removing, and storing under nitrogen.

(*iii*) *Surface Area*

The specific surface areas of the steady-state catalysts were determined by nitrogen adsorption, using a Carlo Erba Series 1800 Sorptomatic and the BET equation.

(iv) X-Ray Diffraction

Diffraction patterns of the steady-state catalysts were obtained using a Siemens 805 diffractometer with 30-KV Cu$K\alpha$ radiation and a nickel filter.

RESULTS

(i) Activity

Results of catalyst activity tests at 595 K are shown in Fig. 1. Results for other temperatures displayed similar behavior; in particular, maximum activity always occurred at the same composition. Activity is presented as a pseudo-first-order rate constant for thiophene disappearance based on unit area of catalyst. Correlation coefficients in obtaining the first-order rate constants from plots of ln $(1 - X)$ vs space time were always greater than 0.99 (X = thiophene conversion). The high degree of apparent first-order correlation is surprising, since extensive kinetic studies generally show inhibition by thiophene and H_2S (e.g., *13–15*). The reasons for this are not clear; it may be an artifact of the use of unsupported catalysts, shallow catalyst beds, and low thiophene initial concentrations (even though conversions covered the range 1–70%). However, as this was not intended to be a kinetic study, this question was not pursued here. All catalysts achieved constant activity within 20 min, and showed no signs of activity decay over test periods of up to 8 hr. The only products of the reaction observed were *n*-butane, 1-butene, *trans*- and *cis*-2-butene. In particular, no butadiene was ever detected. Activation energies and frequency factors were also obtained, and these are shown in Figs. 2 and 3. Correlation coefficients for the Arrhenius plots were better than 0.999.

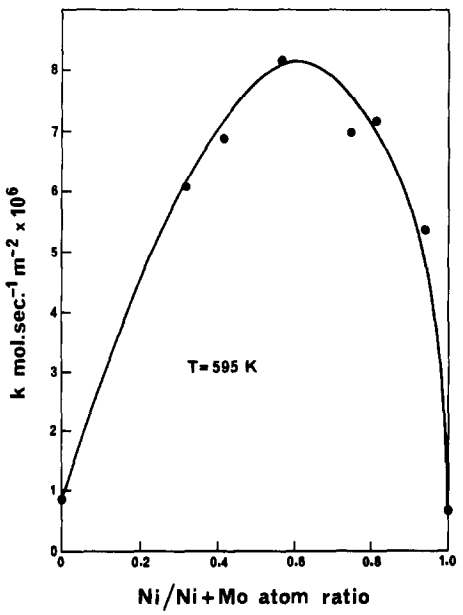

FIG. 1. Activity of catalysts for thiophene hydrogenolysis.

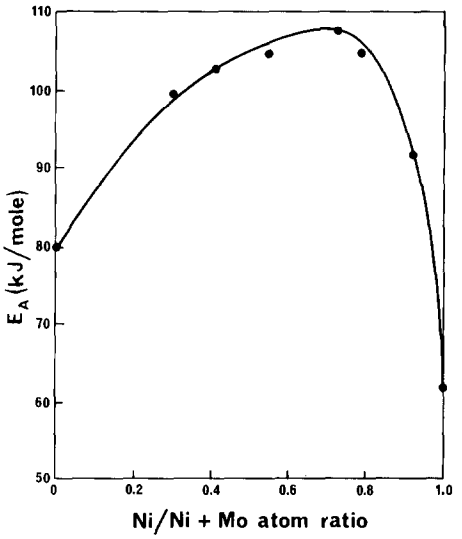

FIG. 2. Apparent activation energies for thiophene hydrogenolysis over various catalysts.

(ii) Surface Areas

Surface areas of the steady-state catalysts are shown in Fig. 4.

(iii) Sulfur Analyses

Sulfur analyses of the steady-state catalysts are shown in Fig. 5.

(iv) X-Ray Analysis

A summary of phase identifications made from diffraction patterns of the various equilibrium catalysts is given in Table 2.

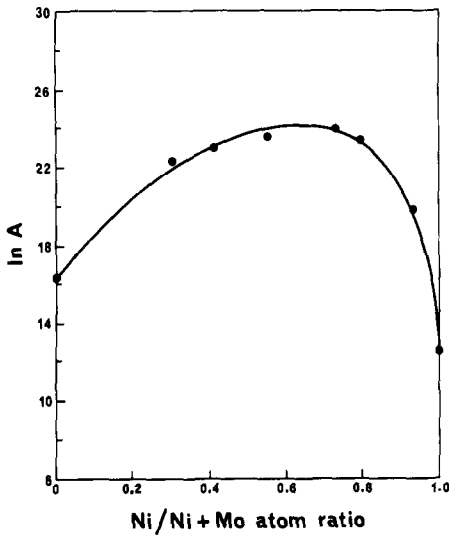

FIG. 3. Frequency factors for thiophene hydrogenolysis over various catalysts.

TABLE 2

X-Ray Analysis of Steady-State Catalysts

Catalyst	Phase	Peak
A	MoO_2	Sharp
B	MoO_2	Sharp
	MoS_2	Broad
C	MoO_2	Sharp
	MoS_2	Broad
D	MoS_2	Broad
	Ni_3S_4	Sharp
E	MoS_2	Broad
	NiS and NiS_2	Sharp
F	MoS_2	Broad
	NiS and β-Ni_7S_6	Sharp
G	MoS_2	Very broad
	NiS and β-Ni_7S_6	Sharp
H	Ni_3S_2	Sharp

DISCUSSION

It is useful to examine the structural results first. X-Ray analysis showed that the nickel-only sample (catalyst H) consisted of well-formed crystallites of Ni_3S_2.

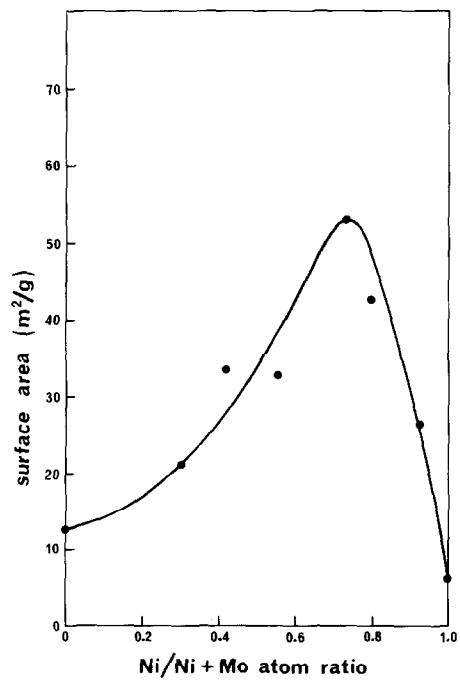

FIG. 4. Surface area of steady-state catalysts.

This phase is expected to be the thermodynamically stable phase under the conditions of the experiments (*16*). The sulfur content of the sample (26.9%) confirmed this result. The Mo-rich samples were characterized by low sulfur contents, and for catalysts B and C, no trace of Ni was detectable by diffraction. The intensity of the 002 peak characterizing the MoS_2 increased with increasing Ni content. The position of the 002 peak remained unchanged over the range of Ni concentration 0–50 atom%. In addition to the phases in Table 2, the high-Ni samples also contained some as yet unidentified phases of nickel. The results of an extensive transmission electron microscope study of the catalysts (*17*) complement these observations. Electron diffraction generally confirmed the X-ray results, and in addition, selected area electron diffraction on catalysts B and C revealed traces of Ni_3S_4. Neither technique found any trace of the mixed sulfide $NiMo_3S_4$ (*18*). Electron micrographs of catalyst A showed crystallites of MoO_2 having an ultimate grain size of some 50 nm, each

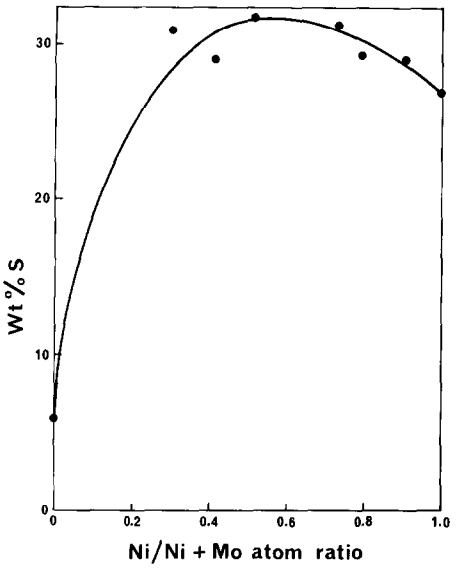

FIG. 5. Sulfur content of steady-state catalysts.

covered with a skin of MoS_2 only 3–4 atomic layers thick. This is perhaps not so surprising in view of the known difficulty of sulfiding bulk MoO_3 (*19, 20*), although it might have been imagined that such small particles should be completely sulfided. Catalyst G likewise showed a skin of MoS_2, several atomic layers thick, over crystals of nickel sulfide, again about 50 nm wide. This result was more surprising. The most active catalyst (D) consisted of highly dispersed, distorted "books" of MoS_2 typically of only 5–6 atomic layers' thickness, together with a few well-formed crystals of Ni_3S_4. Thus the low sulfur content of the Mo-rich catalysts and the broadness of the 002 peaks of MoS_2 are explained. Visually, however, it does not appear that the amount of Ni_3S_4 observed in the electron microscope can account for more than a small portion of the nickel in catalyst D. In any case the sulfur content of a mixture of Ni_3S_4 and MoS_2 containing 55 atom% nickel should be about 41%, whereas only 31.8% was found. It is possible that much of the nickel may be present as fine crystallites of a lower sulfide (or less likely, zerovalent nickel) not detected by diffraction or electron microscopy. Examination of the catalyst in a scanning electron microscope equipped with an elemental analysis facility showed that within the (low) resolution of that instrument, nickel was distributed uniformly throughout the sample. A mixture of Ni_3S_2 and MoS_2 containing 55 atom% Ni would have a sulfur content of about 34.8%. If some allowance were made for edge-intercalated nickel and anion vacancies, then this figure might approach 31.8%. Bulk intercalation of nickel into the MoS_2 could also explain the "lost" nickel and the sulfur deficiency. However, electron micrographs of catalyst D showed that the sulfur layers of the MoS_2 were in perfect registry, suggesting the absence of bulk intercalation. Further, detailed X-ray diffraction analyses showed no change in the C-parameter of the MoS_2. Energetic considerations (*1*) also militate against bulk intercalation of nickel in MoS_2. It is also worth noting that in the case of the highly dispersed MoS_2 (catalyst D), a great number of edges of MoS_2 were present, whereas in the less active catalysts examined (A and G), no edges of MoS_2 were observed.

The surface area of the steady-state catalysts is a strong function of the composition and shows a very pronounced maximum at a nickel content of 0.73. This lies in the region of compositions where the MoS_2 is very highly dispersed. As might be expected from the electron micrographs, the surface area at either end of the composition range is quite low. It is also interesting to note that the surface areas resulting from the method of preparation used here (coprecipitation) are very much higher than those of the two other studies by Furimsky and Amberg (*8*) (impregnation of MoS_2 by Ni) and Thakur *et al.* (*10*) (comaceration).

Turning now to the activity measurements (Fig. 1), we see that catalyst activity displays a pronounced maximum in specific activity located at about 55 atom% nickel. This figure compares favorably with earlier results for supported catalysts (e.g., (*21–23*)), but is somewhat higher than the optimum ratio obtained by Furimsky and

Amberg (*8*) and Thakur *et al.* (*10*) for unsupported catalysts. These differences are almost certainly a result of the method of preparation and the testing conditions. It also suggests that the coprecipitation technique used in this work most closely duplicates the genesis of supported active phases. However, all the work in the area agrees that a comparatively large amount of promoter (>25 atom%) is required to produce optimum activity (e.g., (*4, 8–10, 21, 24, 25*)). This highlights the inadequacies of theories based solely on edge intercalation or semiconductivity effects, which require promoter levels of less than 1 atom% (*5, 9*). While the above mechanisms are possibly operative, a more complete explanation is obviously required. It can also be seen that the catalyst having the highest specific activity has the highest sulfur content. This is contrary to the observations of Massoth and Kibby (*26*) on MoO_3/Al_2O_3 catalysts, and may reflect the influence of the Ni promoter used in this work or the support. Maximum surface area occurs at a higher nickel concentration than that for highest specific activity. This is perhaps not surprising, since it is generally accepted that the catalytically active sites are located at the edges of the MoS_2 layers (*27, 28*), and the BET surface area will therefore include a large area component which is either inactive or has a low activity. It also reflects the dual promoting role of nickel in the unsupported catalyst, i.e., a chemical promoting effect, plus a great influence on the state of dispersion of MoS_2, a fact which appears to have been hardly recognized.

Product distributions showed that the *cis-*/*trans*-2-butene ratio was virtually independent of residence time and catalyst, whereas the butane/butenes ratio increased with increasing residence time. Thus it appears that the isomerization reactions are effectively at equilibrium (in agreement with (*15*)), while the hydrogenation of the monoolefin is a slow step. An interesting observation arises if the total butenes/butane ratio is plotted vs thiophene conversion for all catalysts on one graph. This is shown in Fig. 6. It can be seen that the results for all the mixed catalysts lie approximately on one curve, irrespective of reaction temperature or catalyst. (Only a representative selection is plotted here for clarity.) The results for the pure molybdenum sample (catalyst A) lie somewhat below this line, while those for the nickel-only sample (catalyst H) fall well above it, and are highly temperature dependent. Thus it would appear that the Ni_3S_2 has a lower hydrogenation activity (compared to sulfur removal) than the other systems, and that the hydrogenation reaction on the Ni_3S_2 is more highly activated compared with the desulfurization reaction than on the other catalyst systems. It would also appear that the mixed catalysts resemble more closely the pure MoS_2, as might be expected.

The Arrhenius parameters must be interpreted with some caution when so little is certain about the reaction mechanisms and the rate-controlling steps. However, it would seem that the apparent activation energy for the Ni_3S_2 is quite low, while the catalyst exhibiting the highest activity has a high energy requirement. The activation energies obtained for the most active catalysts (approximately 105 kJ/mole) compare well with the value of 102 kJ/mole obtained by Desikan and Amberg (*29*) for the hydrogenolysis of thiophene over a commercial Co–Mo catalyst. The frequency factor variation suggests that the site density of the optimum formulation is much higher than for either pure sulfide, which might be expected, accepting that active sites are at anion vacancies on the edges of MoS_2 sheets. (These data are not consistent with an alternative interpretation by Stevens and Edmonds (*30*), who suggest that hydrogenolysis sites occur on the basal planes of MoS_2, and hydrogenation sites at the edges.) These observations may also be explained in part by greater errors at either end of the concentration range as a result of

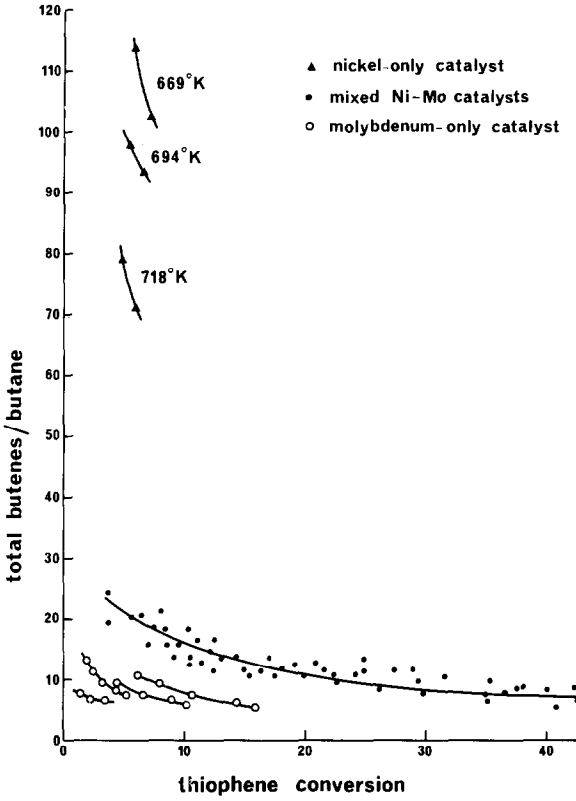

FIG. 6. Total butenes/butane molar ratio versus conversion for all catalysts.

lower conversions. However, the high degree of correlation of the data and the extent of the trend suggest that it is real. The results conform to the well-known "theta rule" when ln A is plotted versus E. However, no particular significance is attached to this.

Present structural theories ascribe the activity of MoS_2 catalysts to coordinatively unsaturated Mo atoms at anion vacancies (*27, 28*). Similar theories have been suggested earlier for the activity of Ni_3S_2 (*31*), although here the emphasis was placed on geometrical arguments, depending upon which planes of Ni_3S_2 were exposed. Such sites would be expected to behave as Lewis acid centers. Accordingly, to see if the frequency factor data could be corroborated, we measured the acidity of the equilibrium catalysts, using ammonia chemisorption at room temperature. The results shown in Fig. 7 were unexpected, and suggest that the total acidity of the pure-nickel catalyst (H) is much higher than the others of the series, and that the optimum formulation catalyst has the lowest acidity (per unit surface area). This appears to be at variance with the ideas above. No real

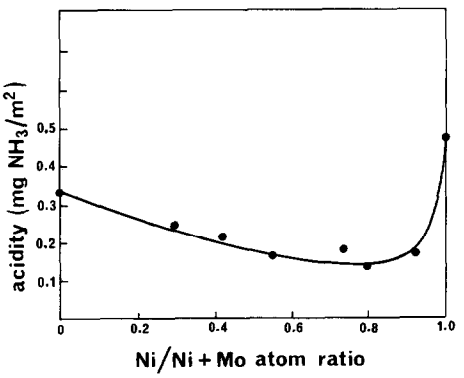

FIG. 7. Surface acidity of various catalysis.

explanation of these results is immediately obvious, although the speculation below may be attempted.

Since we are measuring the acidity of the steady-state catalyst, it is possible that we are detecting acid sites not being used in the reaction process at steady state. If this is so the acidity detected would probably be of low strength. Some credence is given to this idea by the observation that in the ammonia chemisorption experiments, the amount of chemisorbed ammonia fell rapidly as the adsorption temperature was raised. The use of such a strong base as ammonia would be expected to detect even the very weakest sites. We now refer to an early two-site theory of thiophene hydrogenolysis, suggested by Desikan and Amberg (*32*). Using poisoning experiments on a commercial Co–Mo catalyst, they were able to show that two types of acid sites exist; (i) strong sites on which thiophene could be hydrogenolyzed and the product subsequently hydrogenated to butane before desorption, or on which olefins might be chemisorbed and hydrogenated, and (ii) weaker sites on which thiophene was desulfurized only, and 1-butene desorbed either to the gas phase or to migrate to the stronger sites for saturation. The Ni_3S_2 may be suggested to have few strong acid sites (hence the high butenes/butane ratio) and a long tail of weak unused sites (hence the high total acidity). The more active catalysts have a higher proportion of strong and intermediate-strength sites, with few weak enough not to take part in the hydrogenolysis reactions. The low apparent activation energy of Ni_3S_2 may be a result of the sites used for C–S bond scission being of higher acid strength than in the optimal system. Clearly such suggestions are no more than speculation, and more should be known about the distribution of acid strengths on the various catalysts. The apparent high total acidity of Ni_3S_2 may just be a result of complex formation between ammonia and nickel. The nature of the acidity (Brønsted or Lewis) remains unknown in our work, and in addition, some oxidation may have occurred during sample transfer (a sample left in the laboratory atmosphere for several months developed an X-ray diffraction pattern corresponding to $NiSO_4 \cdot 2H_2O$). Further experiments are planned to clarify these points.

The two-site idea of hydrogenolysis of thiophene and subsequent olefin hydrogenation appears to be generally accepted today (*27, 28, 33*). What is unresolved is the nature of these sites. De Beer and Schuit (*27*) suggest that the HDS site consists of a pair of coordinatively unsaturated Mo^{3+} cations at an anion vacancy (reduced from Mo^{4+} by the promoter), while the hydrogenation site would consist of an edge-intercalated Ni^{2+} (although the presence of Mo^{3+} in the operating catalyst has not yet been conclusively demonstrated). This picture would be consistent with the Farragher–Cossee model, but not entirely with the earlier observations of Desikan and Amberg (*32*), nor does it ascribe any role to the nickel or cobalt sulfides, found as a separate phase in operating catalysts (*9, 34*). It might be suggested that olefin hydrogenation occurs on the nickel sulfide. However, this seems unlikely in view of the observations in this work of the lower hydrogenation capacity of the Ni_3S_2 compared to the mixed catalyst. One possible explanation of the fact that all the data points for the mixed catalysts lie approximately on the same line when the butenes/butane ratio is plotted against conversion is that in the actual catalysts, the HDS and hydrogenation sites exist in a near-constant ratio, independent of how much nickel is present as a separate sulfide phase. The tends to suggest that the notion of the two sites consisting of pairs of Mo^{3+} at anion vacancies, and the associated edge-intercalated Ni^{2+} which should be present in an approximately constant ratio (*28*), is intrinsically correct. The reasons for the behavior of the pure Mo sample (catalyst A) are not clear. It would appear to exhibit a higher hydrogenation ability (rela-

tive to the sulfur removal) than the mixed catalysts, and to show a lower apparent activation energy. Few, if any, edges exist in this catalyst, and the occurrence of vacancies in the basal sulfur planes seems less favorable than at edges. At present, it may be tentatively suggested that activity is associated with steps, or other geometrical features arising from the convoluted configuration of the layers in this catalyst, compared to the flakes of the more active mixed catalysts, or that it behaves like a monolayer catalyst (*7*).

It remains to say something of the role of the nickel sulfide associated with the MoS_2 as a separate phase in the most active catalyst. It was suggested above that this is mainly in the form of a highly dispersed lower sulfide, probably Ni_3S_2 at almost atomic dispersion. Both Schuit (*28*) and De Beer and Schuit (*27*) have pointed out the role of the promoter in providing electrons and protons to the MoS_2. However, they are not entirely specific as to whether this task is fulfilled by the intercalated promoter or a bulk form of the promoter. We are inclined to favor the latter. Ni_3S_2 is known to be an *n*-type semiconductor (*35*), and hence cumulative adsorption of hydrogen (as electron donor) will be favored (*36*). Furthermore, addition of electrons to *n*-type Ni_3S_2 by hydrogen adsorption will increase the number of carriers, and hence the conductivity. Thus Ni_3S_2 is uniquely qualified for the task of proton and electron transfer to the MoS_2. In a sense, it could be said that Ni_3S_2 is acting as a "support" for the MoS_2, and that a phenomenon amounting to a "reverse spillover" effect is operating. Hydrogenation of olefins may then occur on the intercalated nickel, which is reduced in the process. The actual hydrodesulfurization involves donation of protons and electrons to the adsorbed S-containing molecule by the MoS_2, during which Mo^{3+} is oxidized to Mo^{4+}. This is then subsequently reduced by the edge-intercalated nickel (*28*).

Wentrcek and Wise (*5*) have shown that for the MoS_2, the rate of the actual HDS reaction is proportional to the number of hole carriers, i.e. predominantly *p*-type semiconductivity is required. Cumulative chemisorption of hydrogen (as an electron donor) should not be favoured on a *p*-type semiconductor. It seems possible that such a mechanism could form the basis of the observed synergy between Ni_3S_2 (or Co_9S_8) and MoS_2, since it would account for the relatively high proportions of promoter required. This explanation apparently also requires Co_9S_8 to be an *n*-type semiconductor. However, no confirmation of this could be found in the literature.

It is worth noting in passing that electronic effects occasioned by the contact of two semiconductors (active catalyst and carrier) have been observed to influence the activation energy of a catalytic reaction (*38*). A similar effect may be responsible for the observed activation energy variation in this work. The rate-determining step may well depend on the relative amounts of the *p*- and *n*-type semiconductors present.

The role of the promoter in sulfide catalyst systems is thus many-faceted. At this stage, it appears that at least the following functions may be suggested for the promoter:

1. Increasing the number of hole carriers in MoS_2 (*5*).
2. Edge-intercalated promoter acts to reduce Mo^{4+} to Mo^{3+} in the catalytic cycle, and may serve as an olefin hydrogenation site, or a point of hydrogen activation (*2, 28*).
3. Control of the dispersion and morphology of the MoS_2, so as to produce highly dispersed flakes with a high proportion of edge sites. The mechanism of this process is not clear.
4. To act as a hydrogen-activating agent through the presence of a separate sulfide phase providing electrons by conduction and protons by migration to the MoS_2. The *n*-type semiconductivity of Ni_3S_2 makes it

well suited to this task. This is possibly the origin of the synergistic effect.

5. Nickel also appears to assist in the reduction of MoO_3 to MoS_2, possibly via a mechanism similar to that in 4 above, and may be connected with the process in 3. A process of electron transfer between promoter and molybdenum during sulfiding has been suggested (*39*).

6. In the case of supported catalysts, nickel has been shown to reduce the formation of $Al_2(MoO_4)_3$, through the competitive formation of a nickel spinel (*40*). A similar function has been suggested for Co (*41*). $Al_2(MoO_4)_3$ is not easily sulfided, thus removing Mo from the catalyst, and is probably an agent in the sintering of the Al_2O_3 support (*16, 40*).

CONCLUSIONS

This work has shown that the reactivity and the morphology of unsupported Ni–Mo sulfide catalysts are critically dependent on the composition. In particular the most active phase, which occurs at about 55 atom% nickel, contains highly dispersed flakes of MoS_2, together with a highly dispersed lower sulfide of nickel, probably Ni_3S_2. It has been suggested that this finely divided Ni_3S_2 being an *n*-type semiconductor would be very well suited for transferring protons and electrons to the MoS_2 by a "reverse spillover" effect, and that this may be a factor in the synergistic mechanism. Product distributions have been interpreted to indicate a constant ratio of HDS sites to olefin hydrogenation sites in the promoted catalyst. This seems to be consistent with the suggestion that HDS sites are coordinatively unsaturated Mo^{3+} cations at anion vacancies on the edges of MoS_2, and that the associated edge-intercalated nickel serves as olefin hydrogenation centers, and to reduce Mo^{4+} to Mo^{3+}, in accordance with the structural model of Cossee and Farragher. Arrhenius parameters and acidity measurements have been obtained, but no satisfactory interpretation of these is possible at present. Whether or not our results are applicable to supported Ni–Mo catalysts is not yet established, though our electron micrographs of used commercial catalysts show the same morphology for MoS_2 as our most active catalysts (*17*). Clearly, however, the unsupported catalyst possesses all the functions exhibited by supported catalysts, viz., C–S bond scission, olefin hydrogenation, and isomerization, though the acidity of conventional supports must be expected to play some role.

REFERENCES

1. Farragher, A. L., and Cossee, P., *in* "Proceedings, Fifth International Congress on Catalysis, Palm Beach, 1972" (J. W. Hightower, Ed.), p. 1301. North-Holland, Amsterdam, 1973.
2. Farragher, A. L., *in* "Symposium on the Role of Solid State Chemistry in Catalysis, New Orleans," *Amer. Chem. Soc. Div. Petrol. Chem. Prepr.* **22**(2), 524 (1977).
3. Grange, P., and Delmon, B. J., *J. Less Common Metals* **36**, 353 (1974).
4. Hagenbach, G., Courty, P., and Delmon, B., *J. Catal.* **31**, 264 (1973).
5. Wentrcek, P. R., and Wise, H., *J. Catal.* **51**, 80 (1978).
6. Schuit, G. C. A., and Gates, B. C., *AIChEJ.* **19**, 417 (1973).
7. Massoth, F. E., *Advan. Catal.* **27**, 266 (1978).
8. Furimsky, E., and Amberg, C. H., *in* "Symposium on the Role of Solid State Chemistry in Catalysis, New Orleans," *Amer. Chem. Soc. Div. Petrol. Chem. Prepr.* **22**(2), 517 (1977).
9. Delannay, F., Thakur, D. S., and Delmon, B., *J. Less Common Metals* **63**, 265 (1979).
10. Thakur, D. S., Grange, P., and Delmon, B., *J. Less Common Metals* **63**, 201 (1979).
11. Andrushkevich, M. M., Buyanov, R. A., Sitnikov, V. G., Itemberg, I. S., and Khramova, G. A., *Kinet. Catal. (USSR)* **14**, 464 (1973).
12. Tamp, N., and Pratt, K. C., *Chromatographia* **12**(8), 527 (1979).
13. Satterfield, C. N., and Roberts, G. W., *AIChE J.* **14**, 159 (1968).
14. Massoth, F. E., *J. Catal.* **47**, 316 (1977).
15. Lee, H. C., and Butt, J. B., *J. Catal.* **49**, 320 (1977).
16. McKinley, J. B., *in* "Catalysis," Vol. V (P. H. Emmett, Ed.), Chap. 6. Reinhold, New York, 1957.
17. Sanders, J. V., and Pratt, K. C., *J. Catal.*, in press (1980).
18. Guillevic, J., Bars, O., and Grandjean, D., *J. Solid State Chem.* **7**, 158 (1973).

19. Massoth, F., *J. Catal.* **36,** 164 (1975).
20. Sotani, N., *Bull. Chem. Soc. Japan* **48,** 1820 (1975).
21. Ahuja, S. P., Derrien, M. L., and Le Page, J. F., *Ind. Eng. Chem. Prod. Res. Develop.* **9**(3), 272 (1970).
22. De Beer, V. H. J., Van Sint Fiet, T. H. M., Engelen, J. F., van Haandel, A. C., Wolfs, M. W. J., Amberg, C. H., and Schuit, G. C. A., *J. Catal.* **27,** 357 (1972).
23. Beuther, H., and McKinley, J., *Ind. Eng. Chem.* **51,** 1349 (1959).
24. Delvaux, G., Grange, P., and Delmon, B., *J. Catal.* **56,** 99 (1979).
25. Canesson, P., Delmon, B., Delvaux, G., Grange, P., and Zabala, J. M., *in* "Proceedings, Sixth International Congress on Catalysis London, 1976" (G. C. Bond, P. B. Wells, and F. C. Tompkins, Eds.), p. 927. The Chemical Society, London, 1977.
26. Massoth, F. E., and Kibby, C. L., *J. Catal.* **47,** 300 (1977).
27. De Beer, V. H. J., and Schuit, G. C. A., *Ann. N.Y. Acad. Sci.* **272,** 61 (1976).
28. Schuit, G. C. A., *Int. J. Quant. Chem.* **12,** 43 (1977).
29. Desikan, P., and Amberg, C. H., *Canad. J. Chem.* **41,** 1966 (1963).
30. Stevens, G. C., and Edmonds, T., *J. Less Common Metals* **54,** 321 (1977).
31. Griffith, R. H., *in* "Advances in Catalysis and Related Subjects" (W. G. Frankenburg, E. K. Rideal, and V. I. Komarewsky, Eds.), p. 91. Academic Press, New York, 1948.
32. Desikan, P., and Amberg, C. H., *Canad. J. Chem.* **42,** 843 (1964).
33. Hargreaves, A. E., and Ross, J. R. H., *in* "Proceedings, Sixth International Congress on Catalysis, London, 1976" (G. C. Bond, P. B. Wells, and F. C. Tompkins, Eds.), p. 937. The Chemical Society, London, 1977.
34. Furimsky, E., and Amberg, C. H., *Canad. J. Chem.* **53,** 2542 (1975).
35. Weissa, O., and Landa, S., "Sulphide Catalysts, Their Properties and Applications." Pergamon, New York, 1973).
36. Stone, F. S., *in* "Chemistry of the Solid State" (W. E. Garner, Ed.), Chap. 15. Butterworths, London, 1955.
37. Germain, J. E., "Catalytic Conversion of Hydrocarbons." Academic Press, New York, 1969.
38. Schwab, G., *in* "Advances in Catalysis and Related Subjects" (D. D. Eley, H. Pines, and P. B Weisz, Eds.), Vol. 27, p. 266. Academic Press, New York, 1978.
39. Ueda, H., and Todo, N., *J. Catal.* **27,** 281 (1972).
40. Laine, J., and Pratt, K. C., Preprints, Sixth Ibero-American Symposium on Catalysis, Rio de Janeiro, 1978.
41. Stork, W. H. J., Coolegen, J. G. F., and Pott, G. T., *J. Catal.* **32,** 497 (1974).